

Active/Passive-Integrated Photonic Crystal Slab μ -Laser

Hideki Watanabe and Toshihiko Baba

We monolithically integrated a μ -laser with a passive waveguide in the photonic crystal slab, for the first time. We demonstrated the lasing operation with light extraction from the waveguide with an external quantum efficiency of 13%/facet.

Introduction: Photonic crystals (PCs) are expected to realize various novel optoelectronic devices. Particularly, the PC slab consisting of a high index semiconductor membrane with holes is a promising platform for advanced photonic ICs due to its strong optical confinement. One of the key issues for photonic ICs based on the PC slab is the monolithic integration of active devices such as μ -lasers [1]-[3] with passive components. However, such integration has never been reported yet. In this study, we successfully fabricated the active/passive-integrated PC slab by using an epitaxial regrowth technique and extracted the laser light from the passive waveguide.

Design: We consider a butt-joint structure of the line defect laser [4]-[6] in the active PC slab and the line defect waveguide in the passive PC slab. The active slab consists of GaInAsP six compressively strained quantum wells and separate confinement heterostructure layers. The total thickness of the slab is 0.21 μm and the emission wavelength is centered at 1.55 μm . The passive slab consists of 1.3- μm -GaInAsP bulk core with the same thickness. The lattice constant a and the hole diameter $2r$ are set to be 0.4 μm and 0.2 μm , respectively. Lengths of the laser and the waveguide are ~ 10 μm and ~ 20 μm , respectively. Fig. 1 shows their photonic bands of the target guided mode, which are calculated with effective indexes of 2.749 and 2.743 for the active and passive slabs, respectively, as the background index n . The laser operation is expected near the photonic band-edge, at which the group velocity becomes zero and a standing wave is formed. For the assumed a , $2r$ and n , the band-edge wavelength λ is adjusted to be 1.55 μm in the μ -laser. If the same parameters are assumed for the waveguide, the photonic band slightly shifts to the higher frequency side, as shown by the dotted curve in Fig. 1, due to the smaller n for the passive slab. On this condition, the laser wavelength would overlap with the cut-off condition of the waveguide. To avoid this, the diameter of holes adjacent to the line defect $2r'$ is reduced, so that the band-edge frequency of the waveguide is lower than that of the laser. Such a band shift is shown by the dashed curve in Fig. 1, where $2r' = 0.9 \times 2r$ is assumed.

Fabrication: For the active/passive-integrated PC slab, two-step epitaxial regrowth technique by metal organic chemical vapor deposition was used. First, the laser wafer including the GaInAsP quantum-well active layer was prepared, and a rectangular mesa was formed by dry etching. Then, the InP layer and the 1.3- μm -GaInAsP bulk core was selectively grown on the etched area, and additionally the InP cover layer was grown on all the area. The air-bridge PC slab was formed by using e -beam lithography, HI inductively coupled plasma etching [7], and HCl wet etching of InP layers. Fig. 2 shows scanning electron micrographs of the fabricated device. The hole diameter $2r$ is 0.20 μm , and the adjacent hole diameter $2r'$ of the waveguide region is 0.18 μm . Although a small projection of 50 nm height is observed on the butt-joint boundary, the active and passive PC slabs are connected with a negligible error of < 10 nm in vertical position. Against this boundary, the position error of the pattern boundary between the laser and the waveguide is less than 1 μm .

Measurement: The room temperature lasing was obtained by pulsed photopumping at $\lambda = 0.98 \mu\text{m}$ with a duty ratio of 0.75%. The laser light from one waveguide facet was directly detected by multimode fiber and observed by optical spectrum analyzer. Fig. 3 shows the lasing characteristics at $\lambda = 1.59 \mu\text{m}$. The effective pump power was estimated from the overlap efficiency η_{ov} of the pump spot to the line defect and the absorption efficiency η_{ab} of the pump light in the slab. As the first approximation, we considered the line defect area to be that inside the innermost holes. Then, η_{ov} becomes 18% for a Gaussian pump spot with a $1/e^2$ diameter of $3.5 \mu\text{m}$. In addition, η_{ab} is estimated to be 30% when assuming a surface reflectivity of 30%, an absorption coefficient of $2 \times 10^4 \text{ cm}^{-1}$ and a slab thickness of 210 nm. It results in a pump efficiency $\eta_{\text{ov}} \times \eta_{\text{ab}}$ of 5.4%, and an effective threshold pump power P_{eff} of $65 \mu\text{W}$. The maximum output power is $5.5 \mu\text{W}$ for $P_{\text{eff}} = 175 \mu\text{W}$ and the corresponding external differential quantum efficiency η_{d} is 13%. To our knowledge, this is the first estimation of the η_{d} for PC μ -lasers.

Conclusion: By using the epitaxial regrowth technique, we successfully integrated a PC slab μ -laser with a PC slab passive waveguide. We demonstrated the laser operation and light extraction with an external quantum efficiency of 13% by pulsed photopumping at room temperature. This work was partly supported by the Grant-In-Aid of JSPS, and the Grant-In-Aid, the IT Program, and the 21st Century COE Program of MEXT.

References

- 1 O. Painter, R. K. Lee, A. Scherer, A. Yariv, J. D. O'Brien, D. D. Darkus and I. Kim, 'Two dimensional photonic bandgap defect mode laser', *Science.*, 1999, **284**, pp. 1818-1821
- 2 H. Y. Ryu, M Notomi, E. Kuramochi and T. Segawa, 'Large spontaneous emission factor ($>0:1$) in the photonic crystal monopole-mode laser', *Appl. Phys. Lett.*, 2004, **84**, pp. 1067-1069
- 3 K. Nozaki, T. Ide, J. Hashimoto, W-H. Zheng and T. Baba, 'Photonic crystal point shift nanolaser with ultimate small mode volume', *Electron Lett.*, 2005, **41**, pp. 843-845
- 4 A. Sugitatsu and S. Noda, 'Room temperature operation of a two dimensional photonic crystal slab defect-waveguide-laser with optical pump', *Electron Lett.*, 2003, **39**, pp.123-125
- 5 K. Inoshita and T. Baba, 'Lasing at band, branch, and intersection of photonic crystal waveguides', *Electron Lett.*, 2003, **39**, pp. 844-845
- 6 W. Zheng, X. Ma, G. Ren, X. Cai, L. Chen, K. Nozaki and T. Baba, 'High efficiency operation of photonic crystal microlaser', *Quantum Electron Laser Sci.*, Long Beach, no. QTuL6, 2006.
- 7 T. Ide, J. Hashimoto, K. Nozaki, E. Mizuta and T. Baba, 'InP etching by HI/Xe inductively coupled plasma for photonic-crystal device fabrication', *Jpn. J. Appl. Phys.*, 2006, **45**, pp. L102-104

Authors' affiliations:

Hideki Watanabe and Toshihiko Baba (Department of Electrical and Computer Engineering, Yokohama National University, 79-5 Tokiwadai, Hodogayaku, Yokohama 240-8501, Japan)

E-mail addresses:

baba@ ynu.ac.jp

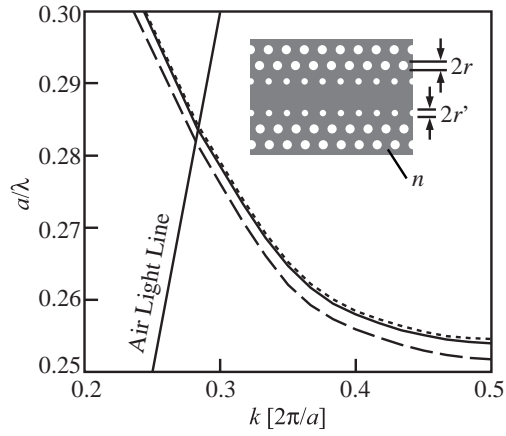


Fig. 1. Calculated photonic bands of fundamental waveguide mode. Solid, dotted and dashed lines denote $2r' = 0.2 \mu\text{m}$ and $n = 2.749$, $2r' = 0.2 \mu\text{m}$ and $n = 2.743$, and $2r' = 0.18 \mu\text{m}$ and $n = 2.743$, respectively.

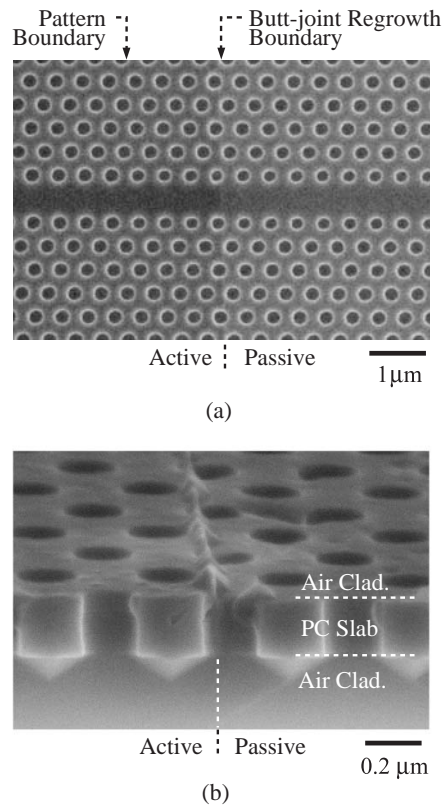


Fig. 2. Fabricated device. (a) Top view. (b) Cross-sectional view.

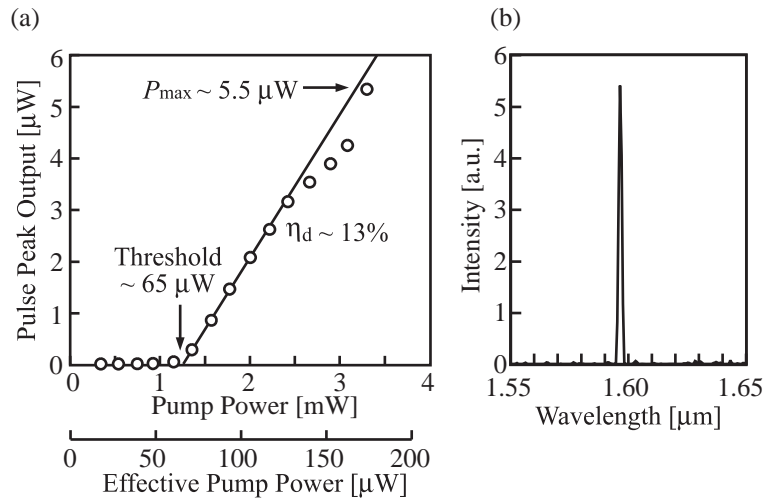


Fig. 3. Observed lasing characteristics. (a) Light output versus pump power characteristic. (b) Lasing spectrum at peak power.